Journal of Alloys and Compounds 508 (2010) 375–379

Contents lists available at ScienceDirect

Journal of Alloys and Compounds

journal homepage: www.elsevier.com/locate/jallcom

Synthesis and characterization of zinc oxide nanorods on silicon for the fabrication of *p*-Si/*n*-ZnO heterojunction diode

R.I. Badran[a,b,*], Ahmad Umar[c,d], S. Al-Heniti[a], A. Al-Hajry[d,e], T. Al-Harbi[a]

[a] Department of Physics, Faculty of Science, King Abdulaziz University, P.O. Box 80203, Jeddah, Saudi Arabia
[b] Physics Department, The Hashemite University, P.O. Box 150459, Zarqa, Jordan
[c] Department of Chemistry, Faculty of Science, Advanced Materials and Nano-Engineering Laboratory (AMNEL), Najran University, P.O. Box 1988, Najran 11001, Saudi Arabia
[d] Centre for Advanced Materials and Nano-Engineering (CAMNE), Najran University, P.O. Box 1988, Najran 11001, Saudi Arabia
[e] Department of Physics, Faculty of Science, Najran University, P.O. Box 1988, Najran 11001, Saudi Arabia

ARTICLE INFO

Article history:
Received 4 June 2010
Received in revised form 30 July 2010
Accepted 4 August 2010
Available online 19 August 2010

Keywords:
ZnO
Nanorods
Photoluminescence
Heterojunction diodes

ABSTRACT

Hexagonal-shaped ZnO nanorods were successfully grown on *p*-silicon substrate via thermal evaporation of metallic zinc powder in the presence of oxygen. The grown nanorods were characterized in terms of their structural and optical properties by using X-ray diffraction, FESEM, HRTEM and room-temperature photoluminescence (PL) spectroscopy. It is confirmed from the observed structural and optical properties, that the grown nanorods are well-crystalline with the wurtzite hexagonal phase and are preferentially grown along the [0 0 0 1] direction and exhibiting good optical properties. The as-grown *n*-ZnO nanorods on *p*-silicon (*n*-ZnO/*p*-Si) substrate were used to fabricate *p*–*n* heterojunction diode which attains a turn-on voltage of ~0.5 V. Temperature-dependant (298, 323, 343, 363, 383, and 423 K) *I*–*V* characteristics for the fabricated diode were also examined and demonstrated in this paper. It was found that the fabricated heterojunction diode was reasonably stable at higher temperatures and the series resistance slightly increases with increasing the temperature.

1. Introduction

Among various semiconductor metal oxide nanostructures, the nanostructure of II–VI semiconductor, ZnO, possesses special place due to its own merits and properties. It is an important *n*-type semiconductor and has various specific properties such as direct and wide band gap (3.37 eV), large-saturation velocity, high-breakdown voltage, high-mechanical and thermal stabilities, large exciton binding energy (60 meV) at room-temperature, etc. The strong exciton binding energy of ZnO compared to thermal energy at room-temperature (26 meV) ensures an efficient exciton emission at room-temperature under low-excitation energy [1–3]. ZnO exhibits biocompatibility hence recently used for the fabrication of various kinds of biosensors [4–6]. Due to the lack of centre of symmetry in ZnO, it exhibits piezoelectric and pyroelectric properties, hence efficiently used for the fabrication of piezoelectric sensors and actuators [7]. In addition to this, ZnO is also efficiently used in various applications such as catalysts, solar cells, field emission devices, sensors and actuators, hydrogen storage, solar cells, electronic and photovoltaic devices, transparent conductive films and so on [8–13]. Because of various excellent properties and so many high-technological applications, variety of ZnO nanostructures have been synthesized by using several fabrication techniques and reported in the literature, to name a few, thermal evaporation process, carbothermal process, vapor-phase transport process, metal organic chemical vapor deposition (MOCVD), arc discharge, solution-based synthesis, template directed wet and dry methods, hydrothermal process, sol–gel process, microwave synthesis process and so forth [1–16]. The ZnO possesses variety of nanostructures, hence it is believed that the ZnO is probably the richest family of nanostructures [1–16]. Few nanostructures of ZnO are nanowires, nanorods, nanocombs, nanonails, nanotubes, flower-shaped and hierarchical nanostructures, nanohelixes, nanosprings and nanorings, doughnuts-like nanostructures and so on [1–26]. Among various nanostructures, the one-dimensional (1D) nanostructure systems such as nanowires, nanotubes, and nanobelts have stimulated much attention due to their unique and specific properties and their applications to nanoscale devices.

In this paper, a very simple and economic method has been demonstrated for the fabrication of hexagonal-shaped ZnO nanorods on silicon substrate. The as-grown ZnO nanorods were investigated in terms of their structural and optical properties. Moreover, the as-grown *n*-ZnO nanorods on *p*-silicon substrate were used to fabricate *p*–*n* heterojunction diode. The temperature-dependant (298, 323, 343, 363, 383, and 423 K), *I*–*V* characteristics

* Corresponding author at: Physics Department, The Hashemite University, P.O. Box 150459, Zarqa, Jordan.
E-mail address: rbadran_i@yahoo.com (R.I. Badran).

0925-8388/$ – see front matter © 2010 Elsevier B.V. All rights reserved.
doi:10.1016/j.jallcom.2010.08.048

of the fabricated diode were also examined and demonstrated in this manuscript.

2. Experimental details

Hexagonal ZnO nanorods were grown in a horizontal quartz tube furnace by using metallic zinc powder and oxygen gas as source materials for zinc and oxygen, respectively. *p*-Type silicon was used as substrate to deposit the ZnO nanorods. Prior to the growth, silicon substrates were cleaned with de-ionized water, methanol and acetone, sequentially and finally dried under nitrogen flow. For the growth of ZnO nanorods, metallic zinc powder was put in an alumina boat and placed at the centre of the quartz tube furnace. The silicon substrates were placed ~7 cm away from the source material. After loading the source material and substrates, the chamber pressure was pumped down to 2–5 Torr using a rotary vacuum pump. After evacuation, the furnace temperature was raised up to 800 °C and oxygen and nitrogen were fed continuously with the flow rates of 100 sccm and 150 sccm, respectively. The reaction was lasted for 2 h and finally white colored products were deposited onto the whole surfaces of the silicon substrate.

The crystallinity and crystal structure of the deposited product were characterized by using X-ray diffraction (XRD) pattern measured with Cu-Kα radiation. To check the general morphologies of the grown nanostructures, field emission scanning electron microscopy (FESEM) was used. For detailed structural characterizations of the grown nanostructures, high-resolution transmission electron microscopy (HRTEM) equipped with the selected area electron diffraction (SAED) pattern was used. The optical properties of the grown nanorods were examined by using room-temperature photoluminescence (PL) spectroscopy. For the *I–V* measurements, "Ag" metal was deposited using thermal evaporation on as-grown ZnO nanorods and Si substrate. The *I–V* characteristics of the fabricated *n*-ZnO/*p*-Si heterojunction diode (0.5 cm × 0.5 cm) were studied by using KEITHLEY 6517A under vacuum using Neytech Qex furnace at 2 Torr at various temperatures (298, 323, 343, 363, 383, and 423 K).

3. Results and discussion

3.1. Structural and optical properties of as-synthesized ZnO nanorods

The crystal phase and crystallinity of the as-grown ZnO nanorods were examined by using X-ray diffraction (XRD) pattern and demonstrated in Fig. 1(a). All the obtained peaks in the pattern are well matched with the reported values of wurtzite hexagonal phase pure bulk ZnO. Except ZnO peaks, no other peaks related to impurities or source material (un-reacted zinc) were found in the pattern (up to the detection limit of X-ray machine) which confirms the formation of wurtzite hexagonal phase for the as-grown ZnO nanorods. A peak positioned at 34.2° assigned as ZnO (0 0 0 2) is highest among other observed peaks in the pattern confirming that the grown nanorods are preferentially grown along the (0 0 0 2) direction.

To know the morphologies and structural properties of the as-grown products, field emission scanning electron microscopy (FESEM) and transmission electron microscopy were carried out and shown in Fig. 1(b)–(d). Fig. 1(a) and (b) demonstrates the typical FESEM images of the grown products which clearly reveal that the deposited structures are hexagonal-shaped nanorods and are densely grown on the whole substrate surface. The typical diameters of the grown nanorods are 125 ± 25 nm. The detailed structural characterizations of the as-grown nanorods were performed by high-resolution transmission electron microscopy (HRTEM) equipped with selected area electron diffraction (SAED) pattern and shown in Fig. 1(d) and (e), respectively.

Fig. 1(d) demonstrates the high-resolution TEM image of as-grown nanorod. The HRTEM image of the nanorod clearly exhibits the distances between two parallel lattice fringes, i.e. about 0.52 nm, equal to the lattice constant of the wurtzite hexagonal ZnO and corresponds to the (0 0 0 1) planes of the wurtzite hexagonal phase ZnO. By this fact, one can confirm that the grown nanorods are well-crystalline with the wurtzite hexagonal phase and grown along the (0 0 0 1) direction in preference. Furthermore, no dislocation or stacking faults were observed from the synthesized ZnO nanorods. Fig. 1(e) exhibits the corresponding selected area electron diffraction (SAED) pattern of the grown nanorods. The observed SAED pattern is well matched and exhibiting the consistency with the HRTEM observation which further affirms that the grown nanorods are well-crystalline with the wurtzite hexagonal phase and grown along the *c*-axis preferred orientation.

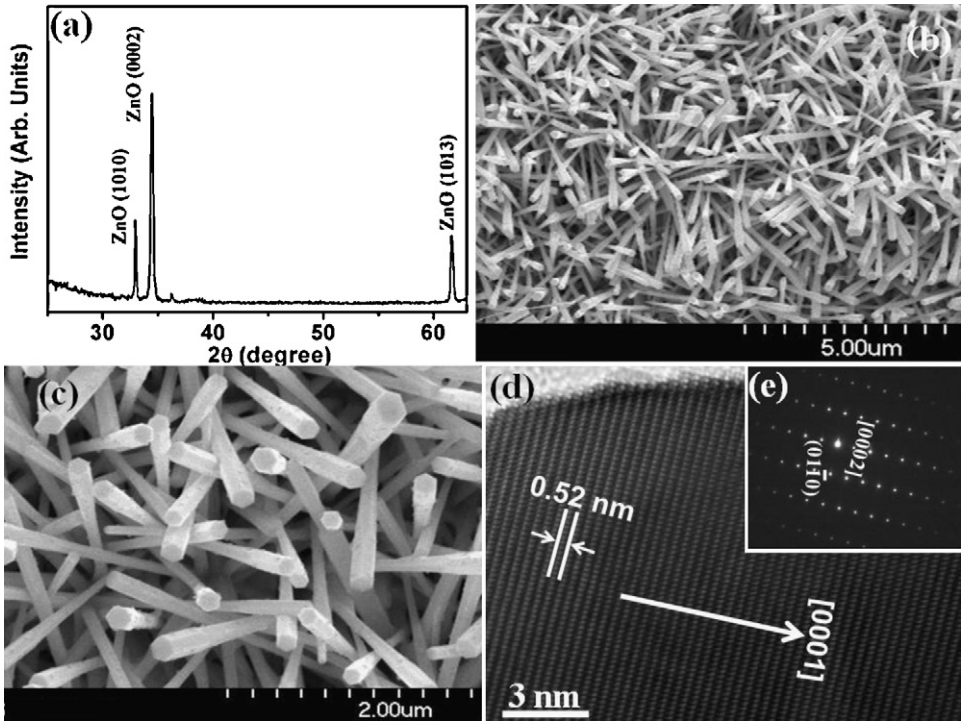

Fig. 1. (a)Typical X-ray diffraction pattern of as-grown ZnO nanorods on silicon substrate, (b) and (c) typical FESEM images, (d) high-resolution TEM image and (e) corresponding SAED pattern of as-grown ZnO nanorods on silicon substrate.

To explain the growth mechanism for the synthesized ZnO nanorods on silicon substrate, the vapor–solid (VS) growth mechanism [19] can be explained instead of commonly and conventionally vapor–liquid–solid (VLS) [20] growth process. In case of VLS mechanism, the source vapor reacted with the catalytic metal particles and formed the alloy droplets. And after attaining the supersaturation state, the grown droplets lead to the formation of nanostructures. It is known that the typical characteristic of VLS mechanism is the presence of metal particles capped at the end of the grown nanostructures. For the growth of ZnO nanorods, no metal nanoparticles or catalysts were used and after the growth no metal particles were found on the tips of the grown nanorods. Hence, one can predict that the growth of ZnO nanorods follows the VS process instead of VLS. In a typical growth process, the Zn atoms were continuously evaporated from the quartz boat during whole reaction process and reacted with oxygen gas in the gaseous phase and form the ZnO vapors. The formed ZnO vapors were deposited onto the silicon substrate in the form of small ZnO nuclei. As the basic characteristic of ZnO is wurtzite hexagonal phase, hence it is predicted that the deposited ZnO nuclei were in the hexagonal shape. Therefore, with increasing the reactant concentrations and reaction time, the deposited hexagonal ZnO nuclei individually grow to upward direction and finally hexagonal-shaped ZnO nanorods were obtained.

The optical property of the as-grown ZnO nanorods was examined by using room-temperature photoluminescence (PL) spectroscopy measured with the He–Cd (325 nm) laser-line as the exciton source and shown in Fig. 2. Generally, two bands have been appeared in the room-temperature PL spectrum of ZnO nanostructures in both UV and visible regions. The peak that appeared in the UV region, also called as near band edge emission (NBE) of the wide band gap of ZnO, is originated due to recombination of free-exciton through an exciton–exciton collision process. Moreover, the peak that originated in the green emission, also known as deep level emission (DLE), is caused by structural defect (zinc interstitials, oxygen vacancies, etc.) and impurities in the deposited nanostructures. Regarding the origination of green emission, the theories given by Vanheusden et al. are generally accepted which stated that the green band in the PL spectrum is generally explained by the radial recombination of the photo-generated hole with the electrons which belongs to the singly ionized oxygen vacancies [21]. A sharp and strong UV emission at ~381 nm and a broad and suppressed green emission at ~522 nm have been observed from the as-grown hexagonal-shaped ZnO nanorods which confirm that the grown nanorods possess good optical properties with less structural defects and impurities.

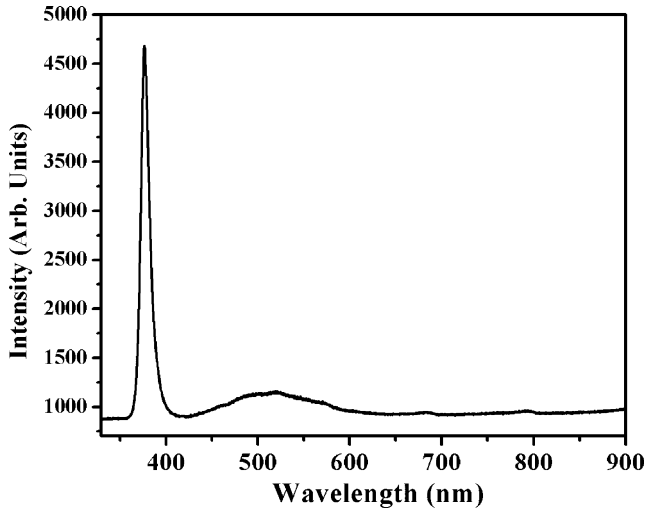

Fig. 2. Typical room-temperature photoluminescence (PL) spectrum of the as-grown ZnO nanorods on silicon substrate.

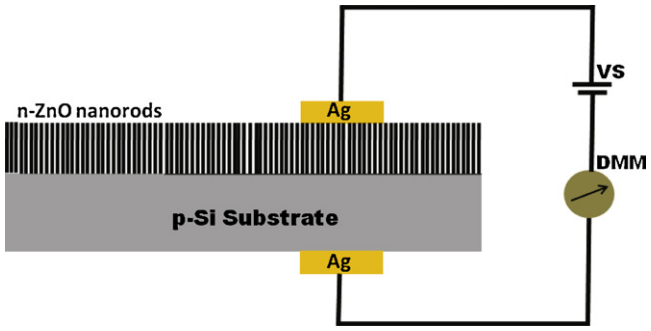

Fig. 3. . Schematic diagram of *p*-Si/*n*-ZnO nanorods based heterojunction diode.

3.2. Electrical properties of the as-synthesized ZnO nanorods

To determine the electrical properties of the as-grown ZnO nanorods, a heterojunction device based on *n*-ZnO nanorods/*p*-Si substrate has been fabricated and their current–voltage characteristics have been examined. The current–voltage (*I*–*V*) characteristics of the fabricated heterojunction diode are studied at several temperatures (from 298 to 423 K) in the forward and reverse bias conditions. Fig. 3 demonstrates the schematic diagram for the fabricated *p*–*n* heterojunction diode made by using *n*-ZnO nanorods grown on *p*-Si substrate.

Fig. 4(a) shows the *I*–*V* characteristics of *n*-ZnO/*p*-Si heterojunction device measured at various temperatures, i.e. 298, 323, 343, 363, 383 and 423 K. The voltage dependence of the junction current

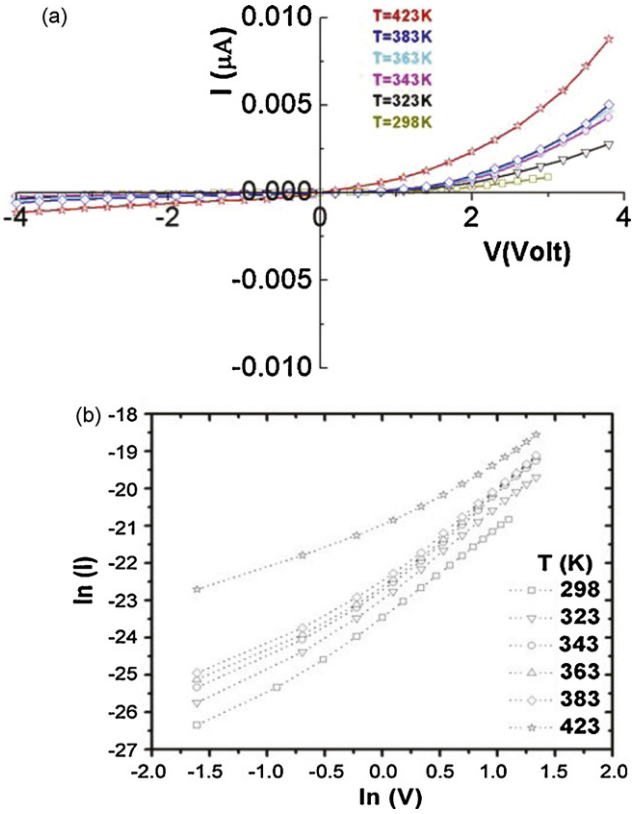

Fig. 4. Typical (a) current versus voltage plots of the *p*-Si/*n*-ZnO nanorods based heterojunction diode at various temperatures (298, 323, 343, 363, 383, and 423 K) and (b) plots of *ln* (*I*) versus *ln* (*V*) at different temperatures for the fabricated *p*-Si/*n*-ZnO heterojunction diode.

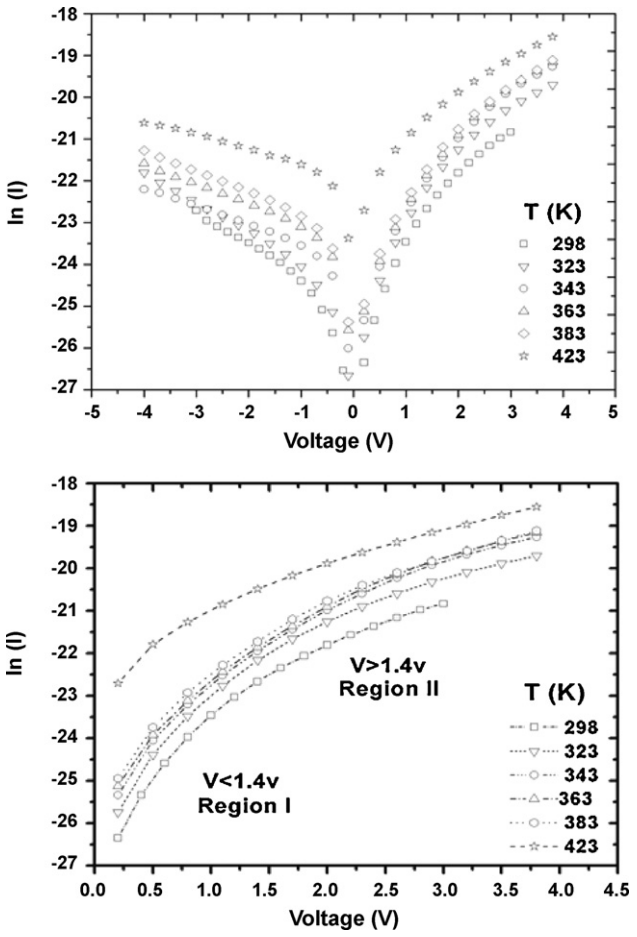

Fig. 5. Plots of $ln\ (I_o)$ versus V for n-ZnO/p-Si device at different temperatures: (a) forward and reverse bias regions and (b) forward bias region indicating different regions of conduction mechanism with different slopes.

may be written as:

$$I = I_o(T)e^{(eV/nkT)}, \quad (1)$$

where, e, k, and I_o (T) are electronic charge, Boltzman constant and temperature-dependent saturation current. Here, n is the quality factor that measures the conformity of the diode to pure thermionic emission. The temperature-dependent saturation current can be related to the effective barrier height V_{eff} by the relation:

$$I_o(T) = AA * T^2 e^{(eV_{\text{eff}}/kT)}. \quad (2)$$

Here, A and A^* are the contact area and Richardson constant, respectively. In a thermionic emission model, a more realistic relation than that shown in Eq. (1) may be adopted and written as [24,25]:

$$I = I_o(T)e^{(eV/nkT)}[1 - e^{(eV/kT)}]. \quad (3)$$

A non-linear and rectifying behavior is obtained in the I–V characteristics of n-ZnO/p-Si heterojunction. The obtained Schottky junction exhibits a diode-like behavior with a turn-on voltage of ~0.5 V, at all temperatures. The obtained turn-on-voltage from the fabricated heterojunction device in our study is close to that already reported in the literature [27,28]. The turn-on voltage allows very small value of current ($\sim 10^{-11}$ A) at all temperatures except at T = 423 K where the device allows a current of $\sim 10^{-10}$ A. Moreover, the low value of current that such device allows, may be due to non-uniform growth geometry of synthesized nanorods. Both, the small gradual change of turn-on voltage and the small change in the slope of forward bias I–V plots via the change in temperature are an indication for attaining a rectifying behavior of the device. The junction, for example at 2.0 V, exhibits a rectifying behavior with rectifying ratio of 6.3. In reverse bias, n-ZnO/p-Si heterojunction diode exhibits small reverse breakdown voltage (~0.55 V) with small reverse leakage current of about 10 pA which can be explained by considering the unique geometry and rod-like morphologies of ZnO nanorods on the p-Si substrates and thus creates more likely a tunneling effect.

Fig. 4(b) demonstrates the $ln\ (I)$ versus $ln\ (V)$ plots for the fabricated p–n heterojunction diode at various temperatures, i.e. 298, 323, 343, 363, 383 and 423 K. The plots clearly demonstrate two regions which have different slopes and may be attributed to two transport mechanisms. The obtained results are in agreement with that reported by Ghosh and Basak [24]. Region I which exhibits a linear dependency of current on the applied voltage may be attributed to a dominated field emission or tunneling mechanism while region II, which shows an exponential relation between the current and the applied voltage, is mainly due to recombination–tunneling mechanism. The mild fluctuations that exist around the slope in region II may be an indication for the stability in the fabricated device. Moreover, it is observed that the second region (region II with $V > 1.4$ V) has an average slope of about three times smaller than that of the first region (region I with $V < 1.4$ V) at all temperatures.

Fig. 5 demonstrates the plots of $ln\ (I)$ versus $ln\ (V)$ for the fabricated p–n heterojunction diode at various temperatures, i.e. 298, 323, 343, 363, 383 and 423 K. The latter plots again show two different regions. From these plots, the intercept and slope can provide the values of saturation current (I_o) and diode quality factor (n), respectively.

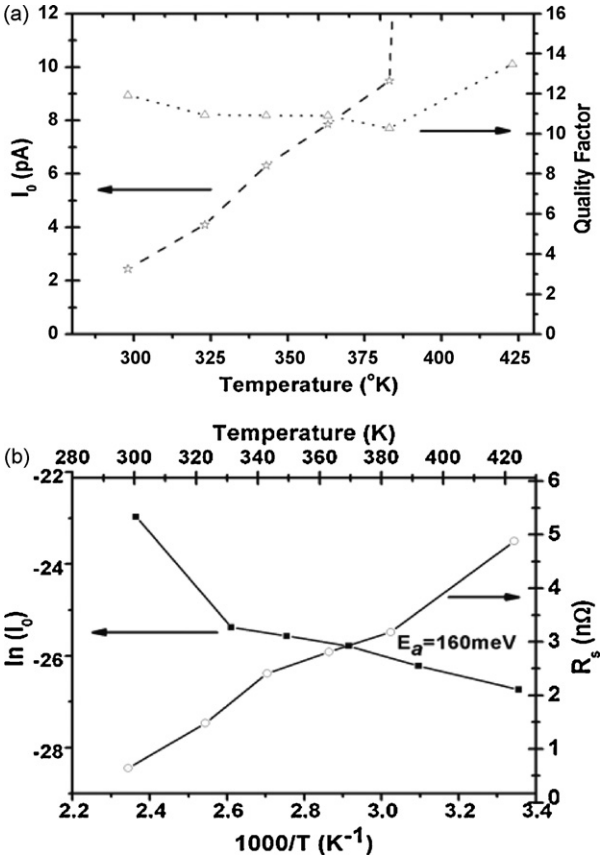

Fig. 6. (a) Saturation current (I_o) and quality factor (n) versus temperature; and (b) series resistance (R_s), versus temperature (T) and $ln\ (I_o)$ versus inverse temperature of the fabricated n-ZnO/p-Si heterojunction diode.

Fig. 6(a) shows the plots for the obtained saturation current and quality factor versus temperature. It is observed, from the plot of saturation current versus temperature, that the saturation current increases with increasing temperature. Similar trend of saturation current with temperature was observed in the data reported in the literature for the *n*-ZnO/*p*-GaN heterojunction diode [27]. Moreover, the quality factor, evaluated at region I, also exhibits similar trend to that observed in the literature [27] when the temperature increases, and apart from a deviation at 423 K temperature, but with a shallower slope. However, *n* exhibits a mild variation around a value of 11 in this region. The values of *n*, in region II, are very much larger than the latter value. Such a trend at higher voltages is in agreement with that shown by others [25]. The high values of *n* at high voltages may be an indication for the existence of high concentration of defect states in ZnO nanorods.

Fig. 6(b) reveals the plot for the variation of $ln\ (I)$ versus inverse temperature. Excluding the point at $T = 423$ K, the activation energy of 160 meV can be extracted from this plot. This latter value is very much larger than the exciton binding energy of ZnO (of about 60 meV). However the global behavior, here, is similar to that obtained in Ref [27]. The series resistance which is obtained from the slope of high voltage region of *I*–*V* plots increases with the increase in temperature and exhibits behavior similar to that found by others [27,29].

4. Conclusions

In summary, *n*-ZnO nanorods were grown on *p*-silicon substrate by simple thermal evaporation process using metallic zinc powder and oxygen gas as source materials for zinc and oxygen, respectively. Detailed structural and optical characterizations confirmed that the grown nanorods are well-crystalline and possess good optical properties. For application view point, the as-grown *n*-ZnO nanorods/*p*-silicon substrate were used to fabricate *p*–*n* heterojunction diode. The fabricated *n*-ZnO/*p*-Si heterojunction diode attained moderate turn-on voltage of ~0.5 V and allowed a current in the order of 10 pA. Temperature-dependant *I*–*V* characteristics for the fabricated device were also examined and presented in this paper. It was observed that the current flow through the device might be dominated by tunneling and recombination–tunneling conduction mechanisms. The obtained results suggest that the simply grown ZnO nanostructures can efficiently be used to fabricate efficient heterojunction diodes.

References

[1] (a) S.J. Pearton, B.S. Kang, B.P. Gila, D.P. Norton, O. Kryliouk, F. Ren, Y.-W. Heo, C.Y. Chang, G.-C. Chi, W.-M. Wang, L.-C. Chen, J. Nanosci. Nanotechnol. 8 (2008) 99;
(b) Z.L. Wang, J. Nanosci. Nanotechnol. 8 (2008) 27.
[2] (a) A. Khan, S.N. Khan, W.M. Jadwisienczak, Sci. Adv. Mater. 2. (2010) 572–577;
(b) D.P. Singh, Sci. Adv. Mater. 2 (2010) 245–272;
(c) R. Ding, J. Liu, J. Jiang, X. Ji, X. Li, F. Wu, X. Huang, Sci. Adv. Mater. 2 (2010) 396–401;
(d) W. Wu, S. Bai, N. Cui, F. Ma, Z. Wei, Y. Qin, E. Xie, Sci. Adv. Mater. 2 (2010) 402–406.
[3] (a) A. Ohtomo, M. Kawasaki, Y. Sakurai, I. Ohkubo, R. Yoshida, T. Yasuda, Y. Segawa, H. Koinuma, Mater. Sci. Eng. B 56 (1998) 263;
(b) S.K. Mohanta, D.C. Kim, B.H. Kong, H.K. Cho, W. Liu, S. Tripathy, Sci. Adv. Mater. 2 (2010) 64–68;
(c) G. Shen, D. Chen, Sci. Adv. Mater. 1 (2009) 213–226;
(d) H. Zhang, N. Du, B. Chen, D. Li, D. Yang, Sci. Adv. Mater. 1 (2009) 13–17.
[4] (a) A. Umar, M.M. Rahman, A. Al-Hajry, Y.B. Hahn, Talanta 78 (2009) 284;
(b) A. Bhardwaj, J.P. Kar, O.P. Thakur, P. Srivastava, H.K. Sehgal, J. Nanosci. Nanotechnol. 9 (2009) 5953–5957;
(c) A. Khan, W.M. Jadwisienczak, H.J. Lozykowski, M.E. Kordesch, Phys. E: Low-dimens. Syst. Nanostruct. 39 (2007) 258–261;
(d) B. Tang, H. Deng, Z.W. Shui, Q. Zhang, J. Nanosci. Nanotechnol. 10 (2010) 1842–1845.
[5] A. Umar, M.M. Rahman, A. Al-Hajry, Y.B. Hahn, Electrochem. Commun. 11 (2009) 278.
[6] A. Umar, M.M. Rahman, S.H. Kim, Y.B. Hahn, Chem. Commun. 166 (2008).
[7] A. Kuoni, R. Holzherr, M. Boillat, N.F. de Rooij, J. Micromech. Microeng. 13 (2003), S103.
[8] H. Zhang, N. Du, B. Chen, D. Li, D. Yang, Sci. Adv. Mater. 1 (2009) 13.
[9] Z.L. Wang, Mater. Today 10 (2007) 20.
[10] X.D. Wang, J.H. Song, J. Liu, Z.L. Wang, Science 316 (2007) 102.
[11] A. Dejneka, A. Churpita, Z. Hubika, V. Trepakov, Z. Potek, L. Jastrabík, G. Suchaneck, G. Gerlach, J. Nanosci. Nanotechnol. 9 (2009) 4094.
[12] A. Umar, B.K. Kim, J.J. Kim, Y.B. Hahn, Nanotechnology 18 (2007), 175606.
[13] A. Umar, M.M. Rahman, Y.B. Hahn, J. Nanosci. Nanotechnol. 9 (2009), 4686.
[14] X.Y. Kong, Y. Ding, R.S. Yang, Z.L. Wang, Science 303 (2004) 1348.
[15] W.I. Park, G.C. Yi, M. Kim, S.J. Pennycook, Adv. Mater. 15 (2003) 526.
[16] K. Huo, J. Fu, H. Ni, Y. Hu, G. Qian, P.K. Chu, Z. Hu, J. Nanosci. Nanotechnol. 9 (2009) 3848.
[17] S. Kim, S. Paek, S. Lee, J. Nanosci. Nanotechnol. 10 (2010) 60.
[18] Y. Song, M. Zheng, L. Ma, W. Shen, J. Nanosci. Nanotechnol. 10 (2010) 426.
[19] A. Umar, Y.B. Hahn, Appl. Phys. Lett. 88 (2006) 173120.
[20] P.X. Gao, Z.L. Wang, J. Phys. Chem. B 108 (2004) 7534.
[21] K. Vanheusden, C.H. Seager, W.L. Warren, D.R. Tallant, J.A. Voigt, J. Appl. Phys. 79 (1996) 7983.
[22] W.I. Park, G.-C. Yi, Adv. Mater. (Weinheim, Ger.) 16 (2004) 87.
[23] C.-X. Wang, G.-W. Yang, H.-W. Liu, Y.-H. Han, J.-F. Luo, C.-X. Gao, G.-T. Zou, Appl. Phys. Lett. 84 (2004) 2427.
[24] R. Ghosh, D. Basak, Appl. Phys. Lett. 90 (2007), 243106.
[25] N. Koteeswara Reddy, Q. Ahsanulhaq, J.H. Kim, Y.B. Hahn, Appl. Phys. Lett. 92 (2008), 043127.
[26] A. Osinsky, J.W. Dong, M.Z. Kauser, B. Hertog, A.M. Dabiran, P.P. Chow, S.J. Pearton, O. Lopatiuk, L. Chernyak, Appl. Phys. Lett. 85 (2004) 4272.
[27] N. Koteeswara Reddy, Q. Ahsanulhaq, Y.B. Hahn, Appl. Phys. Lett. 93 (2008) 083124.
[28] S. Majumdar, S. Chattopdhyay, P. Banerji, Appl. Surf. Sci. 255 (2009) 6141.
[29] N. Koteeswara Reddy, Q. Ahsanulhaq, J.H. Kim, Y.B. Hahn, Explor. Front. Phys. 81 (2008) 38001.